ORIGINAL ARTICLE

Eur. J. Anat. 20 (1): 47-64 (2016)

Sodium azide-induced degenerative changes in the dorsolateral prefrontal cortex of rats: attenuating mechanisms of kolaviron

Olayemi J. Olajide, Busayo O. Akinola, Saliu M. Ajao, Bernard U. Enaibe

Department of Anatomy, College of Health Sciences, University of Ilorin, Ilorin, Nigeria

SUMMARY

Identification of therapeutic targets following neurodegeneration is of major biomedical importance. Kolaviron (Kv) is a biflavonoid complex isolated from seeds of *Garcina kola* – a common oral masticatory agent in Nigeria known to hold medicinal value. Therefore this study evaluated the therapeutic potential of Kv on cells of the dorsolateral prefrontal cortex (DLPFC), before or after sodium azide (NaN_3)-induced neurodegeneration. Rats were randomly assigned into 5 groups (6 each) and treated daily (orally) as follows: 1 ml of corn-oil (vehicle of Kv, 21 days); Kv only (200 mg/kg) for 21 days; NaN_3 only (20 mg/kg for 5 days); NaN_3 (20 mg/kg for 5 days) followed by Kv (200 mg/kg for 21 days); Kv (200 mg/kg for 21 days) followed by NaN_3 (20 mg/kg for 5 days). After treatments, rats were sacrificed and perfused transcardially (with 4% PFA) with brains fixed in accordance with the technique to be used. The DLPFC was examined using histology (H&E), immunoperoxidase (GFAP), immunofluorescence (iNOS & nNOS) and Western blotting (MAPT, MAP2, Bax, BCL-2 and CAD). Quantitative analysis was done using ImageJ software and statistical analysis with Graphpad prism (ANOVA) at $p<0.05$. NaN_3 treatment induced neuronal damage, characterized by reduced relative brain weight, pyknosis, karyorrhesis, astrogliosis, axonal/dendritic damage and cytoskeletal dysregualtion that subsequently resulted in increased expressions of apoptotic regulatory proteins. These degenerative changes were relatable to the observed iNOS and nNOS upregulations. However, Kv administration attenuated the NaN_3- initiated destructive molecular cascades in the DLPFC of rats through mechanisms that involved inhibition of stressor molecules and toxic proteins, prevention of stress related biochemical redox, preservation of neuronal integrity, cytoskeletal framework and subsequently, reduced the level of apoptotic regulatory proteins. We conclude that Kv conferred therapeutic benefits on NaN_3-induced neurodegeneration, particularly when administered before more than after the insult.

Key words: Neurodegeneration – Cytoskeleton – Prefrontal cortex – Kolaviron – Sodium azide

INTRODUCTION

Neurodegenerative disorders (NDDs) affect millions of people every year and is a major cause of long lasting disability that impedes affected individuals from leading a normal life (Enciu et al., 2011). Despite the enormity of the problem, the few therapies available for the management or treatment of NDDs are mostly ineffective (Su et al., 2013). Factors responsible for such failures are multiple. The main challenge is the complexity of these diseases, which has hindered efforts to obtain a comprehensive view of common molecular mechanisms underlying their initiation or propagation (Ebrahimi-Fakhari et al., 2012). However, as research progresses in understanding the molecular mechanisms involved in NDDs, many similarities appear to relate these diseases to one another at subcellular levels (Rubinsztein, 2006). These many parallels between different neurodegenerative dis-

Corresponding author: Olayemi Joseph Olajide. Department of Anatomy, College of Health Sciences, University of Ilorin, Ilorin, Kwara State, Nigeria. Phone: +234 806838 4025. E-mail: llcooly03@yahoo.com or olajide.oj@unilorin.edu.ng

Submitted: 21 September, 2015. *Accepted:* 14 November, 2015.

orders include atypical protein assemblies, oxidative stress, activation of endogenous glia, mitochondrial dysfunction, inflammatory processes and apoptosis (Culmsee and Mattson, 2005; Rubinzstein, 2006; Trushina and McMurray, 2007). Exploring the potentials of a therapeutic target like kolaviron (Kv) with probable inhibitory windows on those similarities offers hope for therapeutic advances that could ameliorate many NDDs simultaneously.

NaN_3 is a substance that is acutely neurotoxic (Smith et al., 1991; Su et al., 2010). Studies carried out to elucidate the compound's mechanism of cellular toxicity implicated it as neuronal mitochondrial toxin (Chang et al., 2011). Selectively reduced complex IV activity is a main pathogenic characteristic of many NDDs, especially in postmortem Alzheimer's disease (AD) brains, and the inhibition of this complex could be evoked by chronic NaN_3 administration in animals (Szabados et al., 2004). Partial inhibition of the mitochondrial respiratory chain produces free radicals, diminishes aerobic energy metabolism and causes excitotoxic damage, creating a deleterious spiral causing neurodegeneration (Liu et al., 2013). Local or systemic administration of NaN_3 induces the release of excitotoxins via mitochondria energy machinery impairment, and this in turn result in neuronal cell loss (Luques et al., 2013). The metabolic and cellular disruptions which can be induced by NaN_3 are also linked with synaptic denervation, cell loss and behavioural deficits in several disease conditions involving NDDs (Marino et al., 2007; Ahmed Mae and Farouk Fahmy, 2013).

On the other hand, Kv is a natural antioxidant and anti-inflammatory bioflavonoid complex, that consists of garcinia biflavonoid (GB1), garcinia biflavonoid (GB2) and kola flavanone in ratio 2:2:1, and is isolated from the seeds of *garcina kola* (bitter kola) (Olaleye and Farombi, 2006; Farombi et al., 2013). It is used as a treatment regimen for several infections and disease conditions owing to its ability as an antiviral, antibacterial and antifungal agent (Farombi et al., 2004). Although a number of useful phytochemicals have been isolated from the seed of *garcinia kola*, the most prominent of them is Kv with a well-defined structure and an array of biological activities including antioxidant, antidiabetic, antigenotoxic and hepatoprotective properties (Farombi and Owoeye, 2011). Previous studies showed that kolaviron is capable of reducing oxidative stress and tissue damage by slowing down the rate of oxygen radical production and stress-related glucose metabolism *in vivo* and *in vitro* (Farombi et al., 2013; Olajide et al., 2015). Despite the available evidence on the antioxidant and anti-inflammatory activities of kolaviron, its therapeutic potentials on brain weight loss, nitric oxide (NO)-mediated neuronal stress, glia activation, interfilament dysfunction (cytoskeleton) and apoptosis in neurodegenerative processes are yet to be elucidated.

The principal aim of the present study was to evaluate and analyze the subcellular neuropathogenic events in the prefrontal cortices of rats following NaN_3-induced neurodegeneration, and to elucidate the therapeutic potentials of kolaviron on such degenerative cascades. Specifically, the objectives of the research were to study changes in: general cytoarchitecture, astrocyte morphology and synapticity, microtubule associated proteins interaction and oxidative redox (considering nitric oxide synthases) in the dorsolateral prefrontal cortex of rats, following NaN_3-induced injury with or without kolaviron therapy. The main significance of the outcomes from this study is that it may provide possibilities of developing potent therapeutic targets, which would be useful in the treatment and management of neurodegenerative disorders. Given that Kv is isolated from a plant that is commonly cultivated, its development into therapeutic targets may present a cheap source of drugs useful especially in third world countries, where many sufferers of NDDs cannot afford the few available, relatively costly, pharmaceutically synthesized drugs. Additionally, despite reports of suicidal and accidental ingestion of the compound, there has been no documented antidote for NaN_3 ingestion. Kv may be useful in such regard also.

MATERIALS AND METHODS

Garcina (bitter) *kola* was procured from a local market in Ilorin, Nigeria. NaN_3 was procured from Sigma-Aldrich (Germany). Phosphate buffered saline (PBS; pH 8.0) was freshly prepared. Antibodies (Rat anti-iNOS, anti-nNOS, anti-GFAP, anti -MAPT, anti-MAP2, anti- Bax, anti-BCL-2 and anti-CAD) were procured from Cell Signalling Technologies, Massachusetts, USA. 3′3′-Diaminobenzidine tetrachloride (polymer) and methenamine silver intensification kits were procured from Sigma-Aldrich (Germany). All other reagents were sourced locally and verified before use as appropriate.

Kolaviron extraction

Seeds of G. kola (GK) were procured from a local vendor in Ilorin, Nigeria and authenticated at the Department of Botany, Faculty of Sciences, University of Ilorin. Kv was extracted from the fresh seeds of GK (4.5 kg) and characterized according to the method of Iwu (1985), as modified by Farombi et al. (2013). To describe the procedure briefly: seeds were pulverized with an electric blender into fine powder. Seed powder was extracted with light petroleum ether (b.p. 40-60°C) in a Soxhlet extractor for 24 h. The defatted, dried marc was repacked and then extracted with acetone and the resultant extract was concentrated and diluted to twice its volume with distilled water and extracted with ethyl acetate (7.250 ml). The

concentrated ethyl acetate fraction gave a yellow solid known as kolaviron.

Treatment solutions

Crystaline salt of NaN_3 (Sigma) was dissolved in distilled water (20 mg/ml) and adjusted to pH 7.4 with 0.1 M phosphate-buffered saline (PBS). This solution was freshly prepared each morning of administration and kept at 4°C before use. Kolaviron was dissolved (40 mg/ml) in corn oil (Carlini®, AL-DI Inc. Batavia) which is the only solvent in which it totally dissolves (Adaramoye et al., 2005; Igado et al., 2012) to allow for oral administration. All treatments were done orally using an oral gavage.

Treatment

Thirty male adult Wistar rats weighing between 180-220 g were assigned into 5 groups (n=6). A group received 20 mg/Kg body weight (BW) of NaN_3 for a duration of 5 days (acute). A separate set were pretreated with 200 mg/Kg BW of Kolaviron (21 days; oral), followed by 20 mg/Kg BW of NaN_3 (5 days) to examine the protective effect of Kolaviron. Similarly, we examined the ameliorative effect of Kolaviron by treating another group with 20 mg/Kg BW of NaN_3 (5 days) followed by 200 mg/Kg BW of Kolaviron for 21 days. A set of control animals received 200 mg/Kg BW of Kolaviron for 21 days while another set received corn-oil only (1 ml at pH 8.0) for 21 days (vehicle for Kolaviron administration). All protocols and treatment procedures were done according to the IACUC guidelines and as approved by the Animal Use in Research Committee of the Postgraduate School, University of Ilorin, Nigeria.

Animal sacrifice and tissue processing

On completion of treatments, rats were euthanized using 20 mg/Kg BW of ketamine (intraperitoneal). Transcardial perfusion was done using 4% paraformaldehyde (PFA) injecting through the left ventricle while the animal was suspended in an inverted position (gravity). Subsequently, brains for histology, immunohistochemistry and immunofluorescence were excised and fixed in 4% PFA overnight at room temperature Cryopreservation was done after 24 hours by transferring the whole brain into 4% paraformaldehyde (containing 30% sucrose) at 4°C in which it was transported to the Research Department of Cell and Developmental Biology, where further processing was carried out. Brains for western blotting were immediately excised after cervical dislocation of rats and transcardial perfusion with PFA. They were transferred into 30% sucrose and rapidly frozen out in liquid nitrogen placed in Thermo-flask container until further processing. Subsequently, coronal sections were made to expose and dissect the dorsal prefrontal cortex (2.6 mm anterior to the bregma) using a Leica dissecting microscope. Following this, the sections were processed routinely to obtain paraffin wax embedded blocks for histology and antigen retrieval immunohistochemistry. Histology paraffin wax embedded sections were stained in Haematoxylin and Eosin using the method of Kiernan (Kiernan et al., 2010).

Immunohistochemistry

Protein cross-linkages were removed in the sections (9 µm thick) by applying 0.1% trypsin for 20 min at room temperature to activate the antigens. Endogenous peroxidase blocking was done using hydrogen peroxide, while 5% bovine serum albumin (BSA) was used to reduce non-specific protein reactions. GFAP primary antibody was diluted (1:100) and applied on the tissue sections (100 µl) for incubation (60 min) at 37°C. Subsequently, secondary biotinylated antibody was desalted and diluted in PBS (pH 8.0) prior to its application on tissue sections. Incubation with secondary antibody was done in the humidity chamber for 30 min at room temperature. Immunogenic reaction was developed using 3′3′ diaminobenzidine tetrachloride (DAB) and intensified using methenamine silver kit (used according to manufacturer's instruction). The sections were counterstained in Haematoxylin, and subsequently treated in 1% acid alcohol to reduce the counterstain intensity.

Immunofluorescence

This was carried out using the method of Fritschy and Hartig (1999). Carefully dissected dorsolateral prefrontal cortices were embedded in optimum cutting temperature (OCT) compound (Thermoscientific). The tissue caskets were dipped into dry ice to freeze out rapidly. For sectioning in the cryostat and staining, the following procedures were carried out: the casket was attached to a mounting chuck with OCT and after dry freezing with dry ice; it was transferred into the cryostat and allowed to equilibrate with the cryostat at 25°C for 30 min. Tissues were sectioned at 15µm and mounted onto Superfrost slides in alternate serial sections. Subsequently, slides were washed 3 x 5mins with 0.1M PBS. Blocking of non-specific proteins was done by incubating the tissue sections for 30 min in blocking buffer (10% calf serum with 1% BSA and 0.1% Triton X-100 in 0.1M PBS). Primary antibodies (anti-iNOS (1:1000); anti-nNOS (1:1000)) diluted in blocking buffer was used to incubate slides overnight at 4°C (Slides were prevented from drying). Slides were then treated with biotinylated secondary antibody (goat anti-rabbit 1:400 in block) and incubated for 2 hours at room temperature. Sections were washed twice with 1% serum PBS for 10 minutes each. Mounting was done using fluoroshield mounting medium (Abcam) and slides were coverslipped. Slides were stored between at 4°C in a covered slide box (covered with foil paper) until examined under the microscope.

Western blotting

Western blotting carried out as described previously Wang et al. (Wang et al., 2006). The steps are summarized thus: Carefully dissected (in ice chamber) dorsolateral prefrontal cortex were harvested and placed in the round bottom microfuge tubes which were immersed in liquid nitrogen to "snap freeze". Per 5 mg piece of tissue, 300 µl of lysis buffer (radioimmuno precipitation assay buffer -RIPA-) was added rapidly to the tube and homogenized with an electric homogenizer. The blade was rinsed twice with another 2x300 µl RIPA buffer and then maintained under constant agitation for 2 hours at 4°C on an orbital shaker in the fridge. Subsequently, centrifugation was done for 20 minutes at 12,000 rpm (4°C) in a microcentrifuge. Supernatants were collected and protein concentrations were determined using Bio-Rad protein assay (Bio-Rad Laboratories, Hercules, USA). The cell lysates with equal amount of proteins (40 µg) were separated by SDS-PAGE and blotted onto polyvinylidene difluoride membranes. The membranes were blocked in Tris-buffered saline with 0.05% Tween-20 (TBS-T) containing 5% non-fat milk overnight. The membranes were then incubated with various primary antibodies (anti-Bcl-2 (1:1000); anti-Bax (1:1000); anti-CAD (1:800); anti-MAPT (1:1000); anti-MAP2 (1:1000) and anti-GAPDH (1:1000)) at 4°C overnight. The membranes were washed 3 times in TBST while agitating for 5 min each time and they were incubated for 1 hour with horseradish peroxidase (HRP)-conjugated secondary antibodies (Jackson ImmunoResearch, West Grove, USA). Images from membranes were developed with Thermo ScientificTM myECL Imager (CCD imager).

Photomicrography and cell count

Histological and immunohistochemical images were acquired using an Olympus binocular research microscope (Olympus, New Jersey, USA) connected to a Cameroscope (5.1 MP). Immunofluorescence images were obtained with the Eclipse 80i Nikon Compound Microscope (Tokyo, Japan) with an attached Hamamatsu DCAM-API digital camera and software (Hamamatsu, Japan). Images from western blot membranes were developed with Thermo Scientific myECL Imager (CCD imager). Histological and Immunohistochemical images were captured at different magnifications as indicated on micrographs and exported to JPEG through which they were analyzed using the ImageJ 1.46r software (National Institute of Health, USA). Cell counting was done using the ImageJ ICTN plugin (cell analyser). Densitometric analysis of blotted proteins was done on digital images using ImageJ software.

Statistical analysis

Statistical analysis Data was analysed in GraphPad Prism (Version 5). Relative average brain weight, cell count outcomes were plotted in ANOVA with Bon Ferroni post-hoc test. Significance was set at $p<0.05$* (95% Confidence Interval). The outcomes were interpreted in a bar chart with error bars; showing the mean and standard error of mean respectively.

RESULTS

General observations and changes in relative brain weight

Generally, it was observed during the experiment that treatment with NaN_3 elicited withdrawal responses in Wistar rats as they immediately abstained from chow, water and the other rats within the same cage/group for about 4 hours. After this period however, the rats returned to normal activities within their cage and also fed on rat chow and water *ad libitum*. Furthermore, it was observed that the overall rate of feed and water intake was not affected by the administration of either corn oil, kolaviron or NaN_3 across the groups. Fig. 1 showed that the relative brain weights of rats in the KV group did not differ significantly from the CO group. Furthermore, it was shown from the result that rats in the NaN_3 group have a significantly decreased relative brain weight when compared with the CO group ($p<0.05$). However, there was a significant increase in the relative brain weights of rats in the NaN_3+KV and KV+ NaN_3groups when compared with the NaN_3 group ($p<0.05$).

Histoarchitectural changes

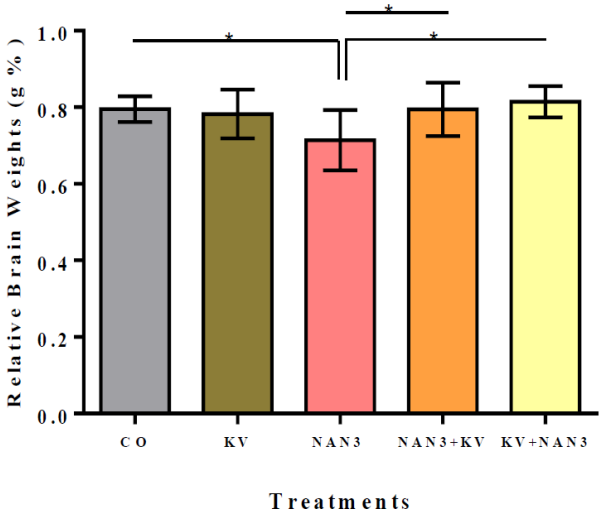

Fig. 1. Bar graph representing the relative brain weights of Wistar rats across the treatment groups. The relative brain weights of rats in the KV group did not differ significantly from the CO group. Rats in the NaN3 group have a significantly decreased relative brain weight when compared with the CO group ($p<0.05$). However, there was a significant increase in the relative brain weights of rats in the NaN3+KV and KV+NaN3groups when compared with the NaN3 group ($p<0.05$).

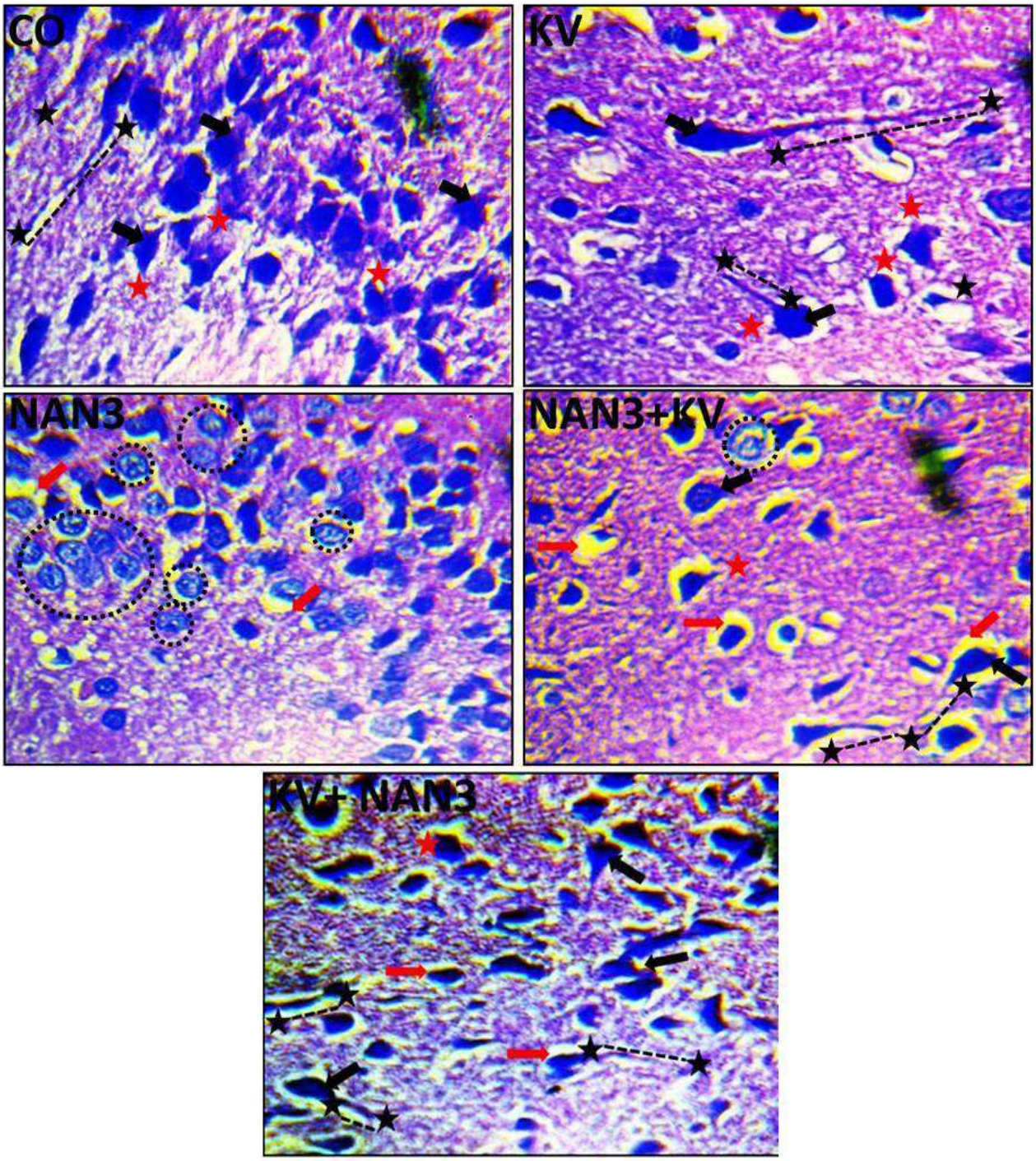

Fig. 2. Representative micrographs of H&E staining showing the general cytoarchitecture of the DLPFC in Wistar rats. Magnification: X400. Normal histological features of the PFC in the CO and KV groups characterized by large pyramidal neurons (black arrow) with long axons (dotted lines between black stars) that extend well from the soma to adjacent neurons within the neuropil. Apical and basal dendrites (red stars) extends from the well delineated soma of the pyramidal neurons in both groups. NaN_3 treatment (NAN_3 group) caused degenerative changes in the PFC that was characterized by clustered pyknotic pyramidal neurons that appear with fragmented cytoplasm and condensed nuclei within soma (dotted circles). Perineural spaces can be seen surrounding degenerating neurons (red arrows) Axons and dendrites are scarcely appreciable around neurons in this group. The NaN_3+KV have a similar morphology with the NaN_3 group but the pyramidal neurons appear larger with considerably longer axons and their nuclei are mostly unfragmented. However, the KV+NaN_3 group is much similar in morphology with the CO and KV groups. The group is characterized by succinctly expressed neurons with appreciable axons and dendrites observable within the neuropil.

Results (Fig. 2) showed normal histological features of the PFC in the CO and KV groups. The histology of these two groups is characterized by large pyramidal neurons with long axons that extend well from the soma to adjacent neurons within the neuropil. Furthermore, short dendritic processes can be seen around the clearly demarcated neuronal perikarya. In the KV group, a few hallospaces created by the neuroglia (particularly oligodendrocytes) which are usually the rounded figures within the neuropil can be appreciated. In contrast however, the NaN_3 group was characterized by various degenerative changes which can be seen all around the neuropil. The degenerative changes in the NaN_3 group include the presence of fragmented neuronal cytoplasm (karyorrhexis) and condensed nuclei (pyknosis), which are shown by the small dotted circles in the photomicrographs. In addition to this, the degenerated pyramidal neurons in this group are cryptic with hardly any visible axons or dendrites within the neuropil. Perineural spaces which surround neuronal soma are also notable features of the NaN_3 group. The histological presentations of the NaN_3+KV group bear some semblance with the NaN_3 group but the neurons appear larger and their nuclei are mostly unfragmented. The morphology of the DLPFC in the KV+NaN_3 group is characterized by succinctly expressed neurons with appreciable axons and dendrites observable within the neuropil. Although a few perineural spaces are present around neurons of the KV+NaN_3 group, the general cortical cytoarchitecture in this group is similar to that of the CO and KV groups.

Glia fibrillary acidic protein (GFAP)

Astrocytes demonstration was carried out in this study using GFAP immunohistochemistry to study its morphology in response to the different treatments. Result showed that the CO and KV groups are characterized by succinctly expressed astrocyte with regular distribution, size and numerous processes which form an array of network within the neuropil (Fig. 3). The neuronal cells in these groups also appeared with normal morphology with several of them seen between and around the branched astrocytic processes. On the contrary, astrocytes integrity in the PFC of rats in the NaN_3 group was disruptively compromised. The disruptive changes include astrogliosis (neurodegeneration-related glia activation) and increased astroglia size which can be seen surrounding pyknotic neurons. Several of the neuronal cells within the reactive astrocytes appear degenerated, with a blebby-like perikarya. Furthermore, the neuropil is generally characterized by several degenerative changes marked by indistinct structural layout of intermediate filaments and halo-spaces between reactive astrocytes. The halospaces appear to have resulted from the migration of reactive astrocytes cleaving degenerating neurons. The NaN_3+KV group have similar astrocyte morphology with the NaN_3 (only) group. The PFC of rats in this group is similarly characterized by reactive astrocytes that can be seen across the entire expanse of the neuropil and are surrounded by pyknotic neurons. However, in contrast to the NaN_3 group, scarred astrocytes as well as some preserved neuronal cells (green arrow) can be seen within the neuropil of the NaN_3+KV group. Astroglia morphology in the KV+ NaN_3 group has very similar appearance with the CO and KV (only) group. In this group, the normal-sized astrocytes are succinctly expressed within the neuropil. Also, many of the neurons between astrocytes have normal morphology without degenerative changes although glia scar can be seen around a seemingly degenerated neuron.

Affectation of the neuronal cytoskeleton

The demonstrated neuronal cytoskeleton and supporting proteins include; microtubule associated protein tau (MAPT) and microtubule associated protein 2 (MAP2) (Fig. 4a). Densitometric analyses of western blotting showed that NaN_3 significantly ($p<0.05$) increased the deposition of MAPT in the DLPFC while pre- administration of Kv neutralized the mean band density of this protein (Fig. 4b). Also, post-administration of rats with Kv following oral NaN_3 treatment did not significantly reduce MAPT over expression. In contrast to MAPT, the density of MAP2 was significantly ($p<0.05$) depleted by NaN_3 treatment in the DLPFC of Wistar rats while Kv intervention after the treatment does not improve this reduction. However, administration of kolaviron to Wistar rats before NaN_3 treatment significantly prevented depletion of MAP2 (Fig. 4c).

Nitric oxide mediated neurodegeneration

Immunofluorescence analysis revealed that NaN_3-induced oxidative stress through excessive synthesis of NO as shown by the increased iNOS immunopositivity in the PFC (Figs. 5a and 5b). Administration of Kv before NaN_3 treatment conferred neuroprotective effects by inhibiting NO overproduction, evinced by the observed reduction of iNOS immunopositivty, and thus inhibiting NO-mediated oxidative stress. However, Kv treatment after NaN_3 held little regulatory effect on NO production. Similar to NaN_3-induced iNOS overexpression, quantitative analysis of nNOS immunofluorescence showed that NaN_3 increased immunopositivity of the enzyme in the PFC of Wistar rats indicating high levels of neuronal NO production (Figs. 6a and 6b). Again, Kv intervention after NaN_3 treatment does not have significant restorative effect on nNOS levels suggesting that it does not totally deplete NaN_3-induced NO overproduction in neural tissue. However, pre-treatment of Kv to rats before NaN_3 downregulated NO production via nNOS.

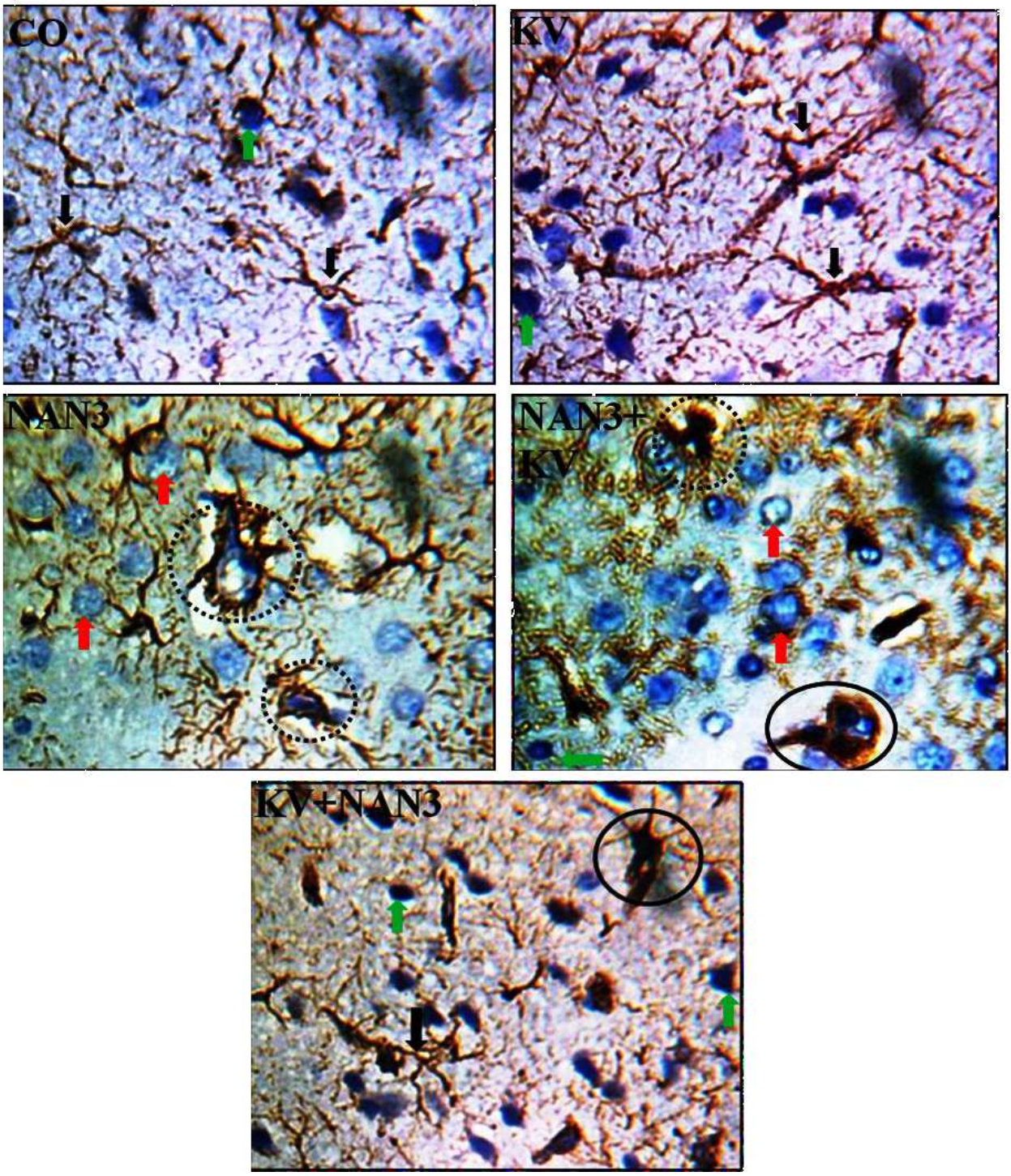

Fig. 3. Representative micrographs of GFAP immunohistochemistry of the DLPFC in Wistar rats. Magnification X400. The CO and KV groups are characterized by succinctly expressed astrocyte with regulardistribution, size and numerous processes which form an array of network within the neuropil (black arrows). Neurons in these groups also appeared with normal morphology (green arrows) with several of them between and around the branched astrocytic processes. On the contrary, activated astroglia (astrogliosis) can be seen surrounding pyknotic neurons (dotted circles) in the NaN_3 group. Neurons appear degenerated across the neuropil in this group as well. Similarly, the NaN_3+KV group is characterized by astrogliosis as in NaN_3 group except for a few scarred astrocytes (solid circles) and some morphologically normal neurons. Astroglia morphology in the KV+ NaN_3 group is very similar in appearance with the CO and KV (only) group. In this group, the normal-sized astrocytes are succinctly expressed within the neuropil and neurons between astrocytes have normal morphology, though glia scar (solid circle) can be seen around a seemingly degenerated neuron.

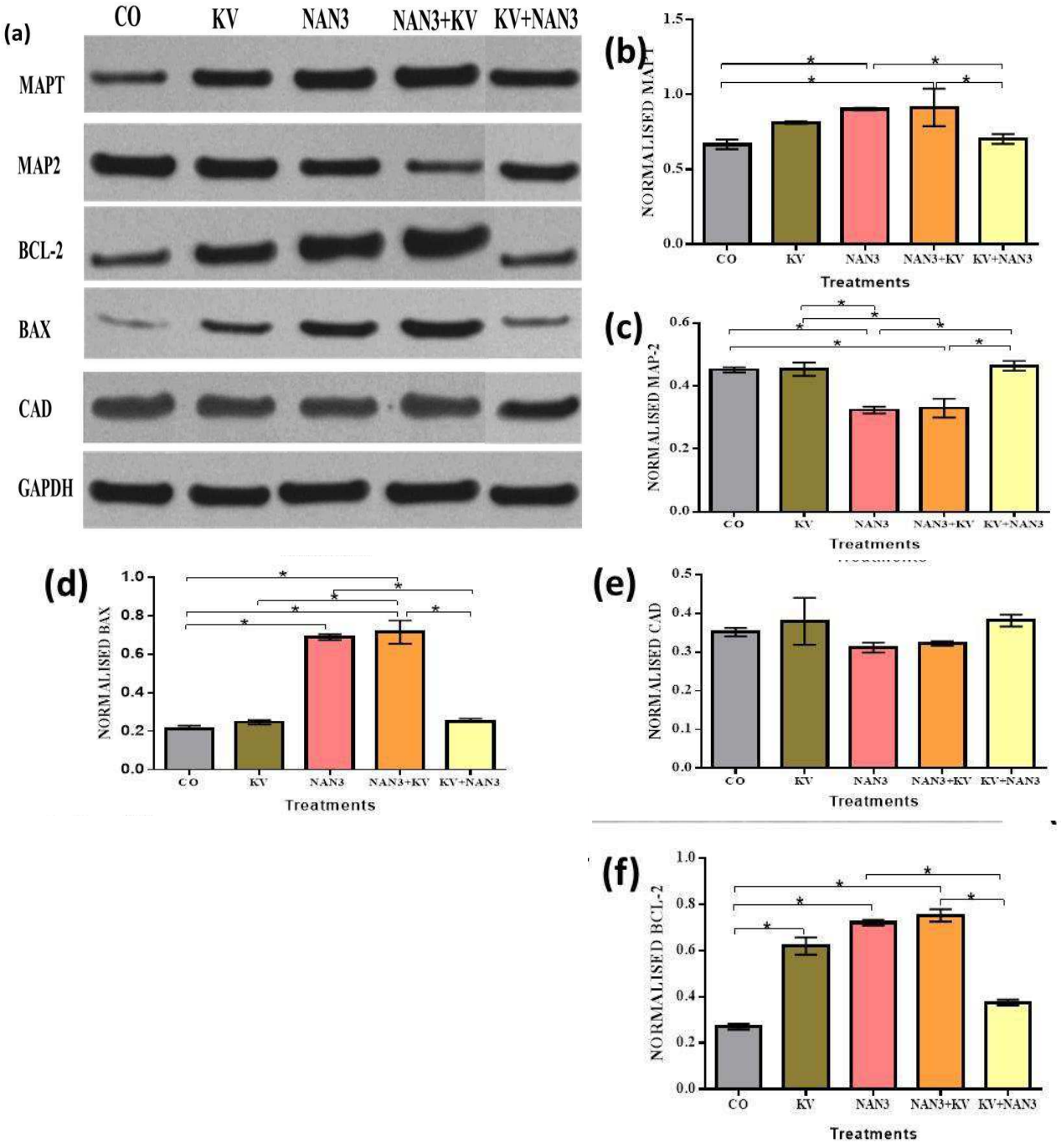

Fig. 4. (a) Western blot analysis of MAPT, MAP2, BCL-2, Bax, and CAD protein levels in cell lysates from DLPFC of Wistar rats treated with the indicated sole or combination of Kolaviron (KV), Corn Oil (CO) and Sodium Azide (NAN_3). Mean band densities of **(b)** MAPT, **(c)** MAP2, **(d)** BCL-2, **(e)** Bax and **(f)** CAD plotted against the loading control (GAPDH). There are observable differences in the densities of blotted protein bands on the polyacrylamide membrane and as shown by densitometric analyses. In MAPT, NaN_3 and NaN_3+KV groups showed a significant increase in MAPT densities when compared with the CO and KV+ NaN_3 groups ($p<0.05$). Similarly, there appear to be an increase in the mean band densities of MAPT in the KV group when compared with the CO and KV+ NaN_3 groups but these were not statistically significant at $p<0.05$. Mean densities of MAP-2 are highest in the CO, KV and KV+ NaN_3 groups. MAP2 in the NaN3 and NaN_3+KV groups showed significant decreases when compared with the other three groups ($p<0.05$). There were statistically significant increase in the mean density of Bax protein in the NaN_3 and NaN_3+KV groups when compared with the CO and KV groups ($p<0.05$). The KV+ NaN_3 group showed a significant decrease when compared with the NaN_3 and NaN_3+KV groups. There was no significant difference in CAD densities across treatment groups at $P<0.05$. For BCL-2, groups treated with NaN_3 and NaN_3+KV respectively showed significant increases when compared with the CO group ($p<0.05$). Both the NaN_3 and NaN_3+KV groups showed significant increment in BCL-2 density when compared with the KV+NaN_3 group ($p<0.05$). Surprisingly however, the KV group also showed a significant higher BCL-2 density when compared with the CO group ($p<0.05$).

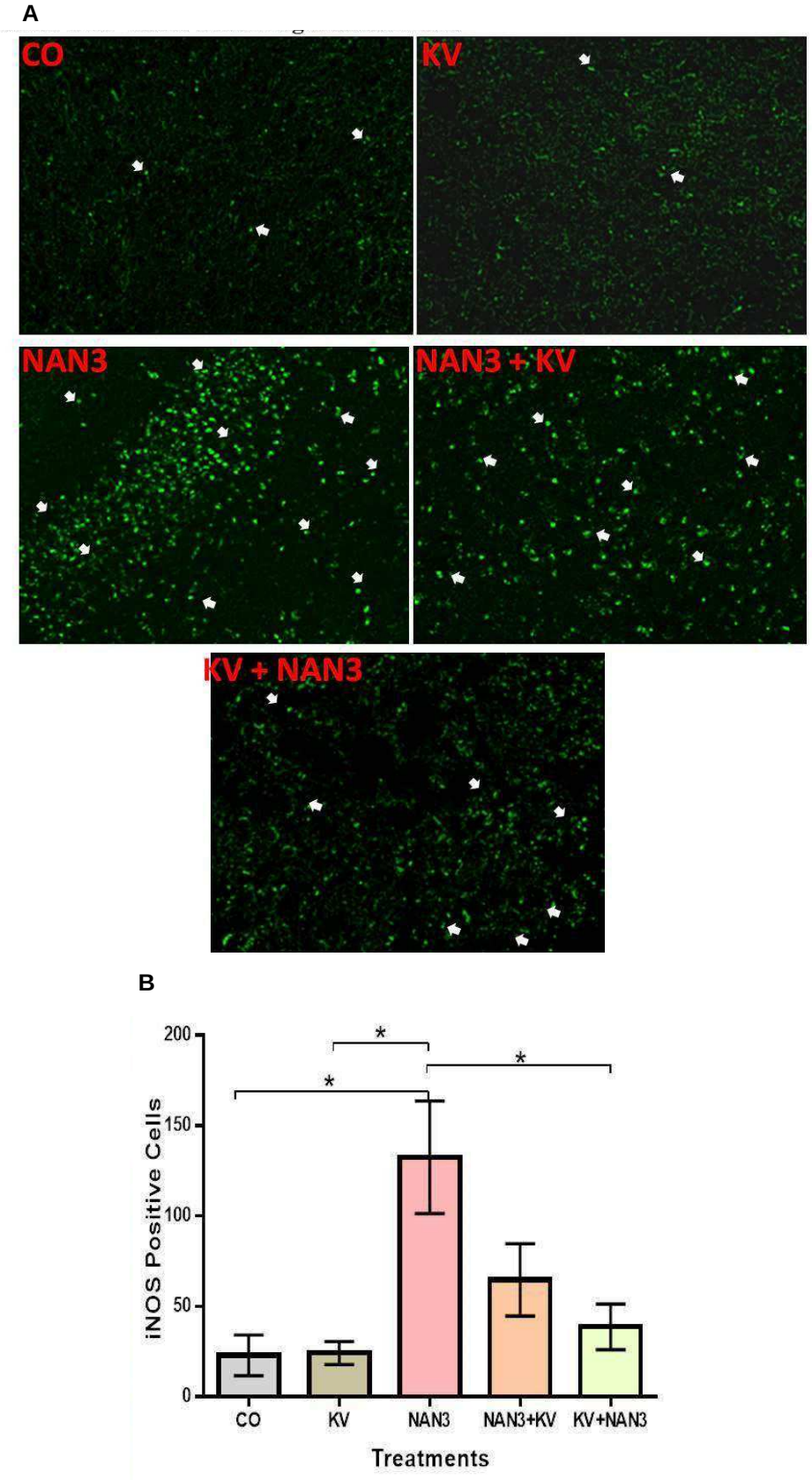

Fig. 5. (A) Representative micrographs showing immuno-expression of inducible nitirc oxide synthase (iNOS) in the DLPFC of Wistar rats. Magnification: x40. **(A)** iNOS expression in the treatment groups is significantly different. **(B) Expression of iNOS Immuno-positive cell count for different treatment groups.** *=p<0.05. The increase in iNOS positivity in the NaN3 group is significantly different from that in the CO, KV and the KV+ NaN_3 groups (p<0.05). The NaN_3+KV group does not differ significantly from the NaN3group at p<0.05. However, the NaN_3+KV group does not differ from the other treatments group also.

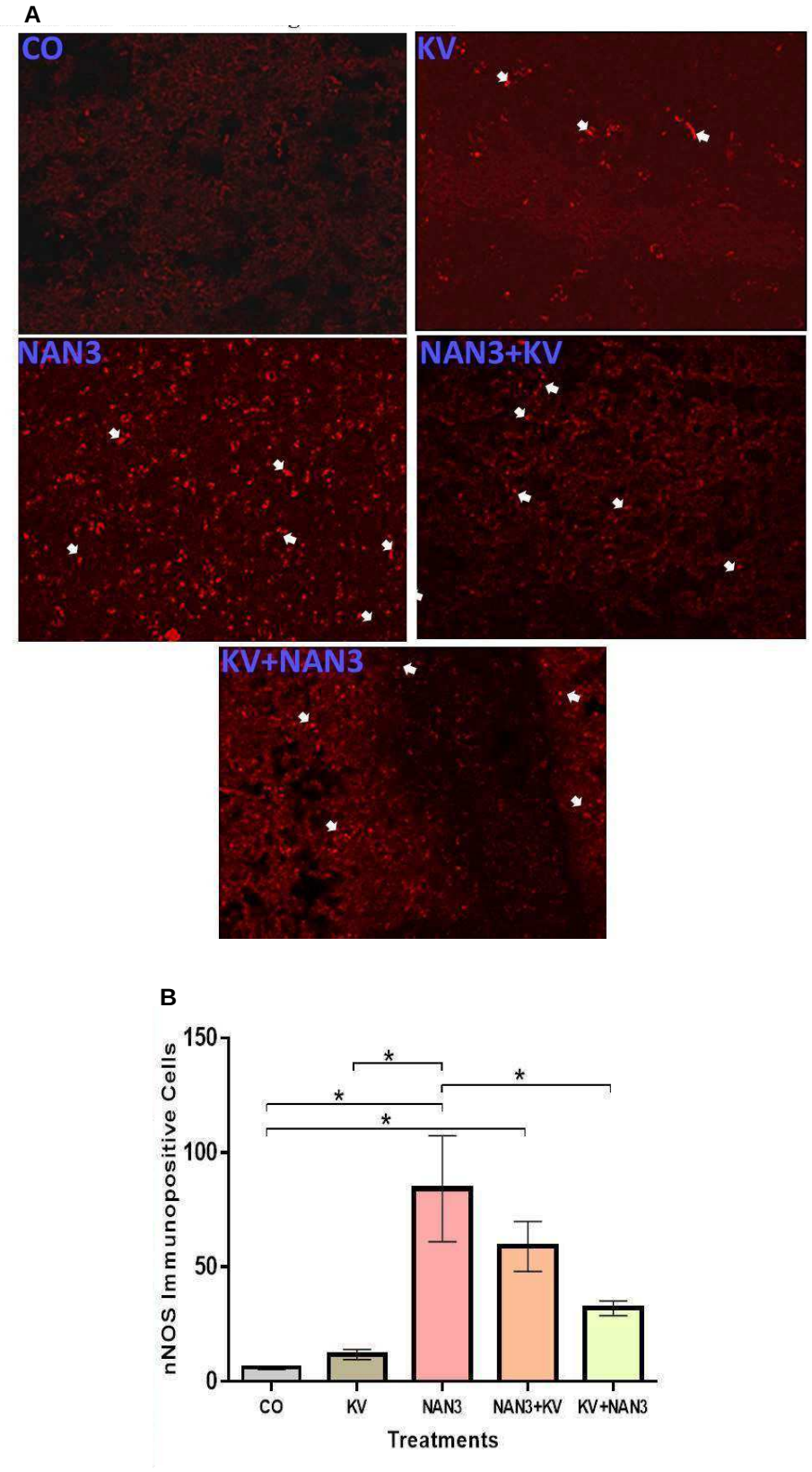

Fig. 4. (A) Representative micrographs showing immuno-expressions notric synthase (nNOS) in the DLPFC of Wistar rats. Magnification:X40. nNOS positivity in the NaN_3 group is increased compared with the CO, KV and the KV+ NaN_3 groups ($p<0.05$). **(B) Expression of nNOS Immuno-positive cell analysis for different treatment groups.** *=$p<0.05$. The bar graph revealed that there was a significant increase in nNOS expression in the NaN_3 when compared with the CO, KV and KV+ NaN3 group $p<0.05$. There appeared to be a reduction in nNOS expression in the NaN3+KV group when compared with the NaN_3 group but this was not significant at $p<0.05$. Also, the NaN_3+KV group showed a significant difference from the CO group.

Cell cycle regulating (apoptotic) protein dysfunction

Apoptotic regulatory proteins including Bax, CAD, BCL-2 were studied (Fig. 4a). Two pro-apoptotic proteins (BCL-2 associated X protein (Bax) and Cathepsin D (CAD)) and an anti-apoptotic protein (BCL-2) were immuno-blotted. The result revealed increased Bax expression by NaN_3 administration, and this was significant at $p<0.05$ wherein the mean band density of Bax protein significantly increased in the NaN_3-treated rats, when compared with the other groups (Fig. 4d). The result further showed that Kv intervention before but not after prevented such increment. The lysosomal protease CAD did not show any significant difference in mean band densities of the protein across treatment groups (Fig. 4e).

Surprisingly, NaN_3 also significantly increased the mean band density of anti-apoptotic protein BCL-2 in the PFC of Wistar rats. However, treatment of rats with Kv (only) also showed a significant higher BCL-2 density when compared with rats treated with corn oil. In addition, pre-administration of Kv significantly prevented NaN_3-induced neuronal BCL-2 increment whereas post-administration of Kv to does not prevent increased BCL-2 expression in rats (Fig. 4f).

DISCUSSION

Altered average brain weight

A number of studies evaluating brain tissue volumes or metabolic function in NDDs are demonstrating that regional tissue loss and hypometabolism correlate with specific cognitive and behavioural impairments in ways that are similar to what has been seen with other more focal types of pathology (Navarro and Boveris, 2010). One of the manifestations of NaN_3-induced toxicity as shown from this study is altercation in the brain weight of treated rats. 20 mg/kgBw of NaN_3 was shown to significantly reduce the relative brain weights of Wistar rats. This characteristic reduction in brain weight induced by NaN_3 is similar to the manifestations of several NDDs pathology. Reduced relative brain weight has been linked to abnormal neurochemistry, which is synonymous with abnormal functionality in sections of the brain. As an example, decreased serotonin, 5-hydroxyindoleacetic acid and dopamine were detected in the cortex and the hypothalamus of adult mice with reduced relative brain weight (Mercer et al., 2009). In addition, decreased brain weight and volume have been observed in leading brain disorders including Schizophrenia, Alzheimer's, Parkinson's, Huntington's diseases (Farzan et al., 2010; Van Laar and Berman, 2013). Furthermore, like NaN_3, some neurotoxic agents are also known to exert brain damage by selectively reducing brain weight (Cecil et al., 2008). It is suggestive that adverse brain weight outcomes induced by NaN_3 in this study may be related to metabolic impairment and persistent excitotoxicity. In support of this, frontal lobe white matter reduction was reported to result directly from the neurotoxic effect of abused drugs that include cocaine, heroin and cannabis and this was directly linked to inhibition of the process of myelination leading that subsequent led to degeneration (Schlaepfer et al., 2006). Additionally, results from this study showed that pre- treatment of rats with 200 mg/kgBw Kv, before NaN_3-treatment significantly prevented a reduction in relative brain weight. Recent studies have suggested that consumption of diets rich in such therapeutic components as antioxidants and anti-inflammatory, like Kv may lower the risks of age-related loss of brain volume that result in cognitive declines and increased risk of NDDs (Joseph et al., 2009). However, in contrast to the significant and definitive role of Kv against relative brain weight loss, findings from the present study revealed that Kv intervention after NaN_3 neurotoxicty holds very little restorative effect on the reduced brain weight. This suggests that although Kv administration following NaN_3-induced neurotoxicity may have effected reduction of the neurochemical imbalances that orchestrated brain weight loss, it had limited therapeutic potentials at halting the NaN_3-induced neurotoxicity entirely; hence the recorded brain weight loss in the neuroreparative group. This observation supports the notion that Kv's protective mechanisms against brain weight loss was by delaying or halting progressive degeneration of the involved neurochemical pathways. Such neuroprotective mechanism has been proposed as a causal therapeutic strategy for Parkinson's disease (PD), AD, and amyotrophic lateral sclerosis (Nieoullon, 2011).

NaN_3-induced histomorphological disruption and Kolaviron therapy in the PFC

The cellular anatomy of the control groups (corn oil (CO) and kolaviron only (KV)) were dominated by large pyramidal neurons (characterized by their distinct apical and basal dendritic trees and the pyramidal shape of their soma), with long axons, that extended well to adjacent neurons within the neuropil. The observed neuronal, axonal and dendritic morphology in these groups, suggests appropriate and normal functionality of the DLPFC, since from the functional point of view, the neurons are the most important cells of the brain (Coward, 2013). Together with the dendrites, the axons form the synapses, through which signals are sent from the axon of one neuron to a dendrite of another (Major et al., 2013). As observed in the histoarchitecture of the CO and KV groups, the well-extended axons of pyramidal neurons and the demonstrated dendritic processes connote suave synaptogenesis within the DLPFC in these groups. NaN_3–induced cytoarchitectural damage present-

ed with properties of early stage apoptosis as apoptotic cells are characterized by cell shrinkage and pyknosis (Osten and Margrie, 2013). On histologic examination with H&E staining, apoptosis involves single cells or small clusters of cells (as shown by the dotted circles around the degenerating neurons in the NaN_3 group from Fig. 1 (KV & CO), and the apoptotic cell appears as a round or oval mass, with dark eosinophilic cytoplasm and dense purple nuclear chromatin fragments. Furthermore, the cryptic changes seen in the soma of pyramidal neurons in the NaN_3-group also suggests apoptotic mode of neuronal cell death, in which cell shrinkage made the cells smaller in size, with dense cytoplasm and the organelles more tightly packed. Similarly, neuronal apoptotic bodies have been described to consist of cytoplasm with tightly packed organelles, with or without a nuclear fragment (Stefanis et al., 1997). Another hallmark characteristic of apoptotic neurons in the NaN_3-treated rats in this study is defective axons which definitely will lead to loss of synaptogenesis. Defective axons are not only present in diseased neurons, but they also cause certain pathological insult due to accumulation of organelles (Coleman and Freeman, 2010). The subject of reduced or lost neural communication from defective axons in this study is further supported by the presence of perineural spaces which were seen to surround the neuronal soma in the NaN_3 treatment group. Therefore, it is suggestive that structural alteration in axonal morphology caused by NaN_3, led to loss of signal processing, neuronal timing and synaptic efficacy in the PFC of rats, which may also account for the tissue weight alterations seen in this study. However, 200 mg/kgBw of Kv showed partial restorative potential against NaN_3-induced neuronal cell death, when administered after treatment with NaN_3, The neurons in this group appear larger and their nuclei are mostly unfragmented. However, the cyto-protective property of Kv was pronounced in the group in which it was given before NaN_3. The morphology of the PFC in this group was characterized by succinctly expressed neurons, with appreciable axons and dendrites observable within the neuropil. Although a few perineural spaces are present around neurons of this group, the general cortical cytoarchitecture is much similar to that of the CO and KV groups. Kv neuroprotective mechanism against neuronal death may be through the inhibition of NaN_3-activated neuronal biochemical cascades that trigger proteases which destroy molecules that are required for cell survival and others that mediate a program of cell suicide in neuronal apoptosis. These shown potentials of Kv are important, as apoptotic mode of neuronal cell death is reportedly the predominant from of cell death in chronic NDDs (Friedlander, 2003; Elmore, 2007) and axonal dysfunction in the nervous system, has been shown to be one of the major causes of several NDDs (De Vos et al., 2008).

Neuronal cytoskeletal and support protein dysfunction and Kolaviron protective mechanisms

Dysfunction of neuronal cytoskeletal and support proteins are neuropathological signatures of many NDDs, and mutations in these proteins have been implicated in the pathogenic cascades involved in neurodegenerative processes (Cairns et al., 2004). The morphology of astrocytes, which confer both structural and metabolic support on neurons, was demonstrated using GFAP immunohistochemistry. Also, microtubule associated protein Tau (MAPT) and microtubule associated protein 2 (MAP-2) which are involved in both axonal growth and support were demonstrated using western blotting techniques.

Reactive astroglia (astrogliosis) and Kolaviron intervention

Since astrocytes regulate neural circuit function in the healthy and diseased brain, studying astrocyte morphology is key to the development of therapeutic agents to treat these diseases (Clarke and Barres, 2013). With the treatment duration adopted in this study, GFAP immunohistochemistry revealed no major change in astrocyte distribution and structure, in both the CO and KV groups as they are characterized by succinctly expressed astrocyte, with regular sized and numerous processes, which form an array of network within the neuropil. The normal morphology of astrocytes would have made numerous essential contributions to normal functions, including regulation of blood flow, provision of energy metabolites to neurons, participation in synaptic function and plasticity, and maintenance of the extracellular balance of ions, fluid balance and transmitters (Sofroniew, 2009).

On the contrary, as a result of the NaN_3-induced neurotoxicity in this study, astrogliosis (neurodegeneration-related glia activation) associated with degenerative (pyknotic) neurons and inflammatory processes occurred in rats. The mechanisms that lead to astrogliosis are not fully understood. However, damaged neurons have long been reported to induce astrogliosis and astrogliosis has been used as an index for underlying neuronal damage (Zhang et al., 2010). Furthermore, the neuropil was generally characterized by indistinct structural layout of intermediate filaments and halo-spaces between reactive astrocytes. The halo-spaces appear to have resulted from the migration of reactive astrocytes cleaving pyknotic neurons. Such changes in molecular expressions undergone by astrocytes as they become reactive have the potential to deplore pronounced effects on surrounding neural cells. In similarity with GFAP findings from this study, Megyeri et al. (2008) showed pathological changes in the ultrastructure of mitochondria and glial cells, detected

in NaN_3–treated animals suggesting its ability to disrupt the blood–brain barrier. Many studies have also shown that astrogliosis is one of the principal events associated with most NDDs resulting from damage by oxidative stress (Triolo et al., 2006). Thus, it is inferred that the observed astrogliosis and degenerative formation of astrocytes seen in this study are a result of NaN_3-induced oxidative stress and inflammatory processes. The group of rats treated with NaN_3 before kolaviron therapy (NaN_3+KV) had similar astrocyte morphology with the NaN_3 (only) group. The DLPFC in this group is similarly characterized by reactive astrocytes and pyknotic neurons across the entire expanse of the neuropil. However, in contrast to the NaN_3 group, scarred glia as well as a number of morphologically normal neurons are within the neuropil of this group. These findings further buttress earlier observations of the partial restorative role played by kolaviron against NaN_3-induced neurotoxic processes from oxidative stress. Increasing evidences suggests a beneficial role for this scar tissue as part of the endogenous local immune regulation and repair process for degenerating neurons (Rolls et al., 2009). Neurons with normal morphology found around the glia scars suggest the role of observed scar formation in neural repair processes. Furthermore, there are strong evidences that mature astrocytes can re-enter the cell cycle and proliferate during scar formation (Buffo et al., 2008), this may explain the mechanisms by which kolaviron initiated restorative effects on degenerative neurons caused by NaN_3 treatment in this study.

Astrocytes morphology in the group treated with kolaviron before NaN_3 has very similar appearance with those of the control groups. This buttresses that a neuroprotective mechanism of kolaviron in preventing neuronal cell loss in this study is through prevention of astrogliosis. This can be linked to its strong inhibitory properties against oxidative stress and proinflammatory proteins, which possibly propagated the toxic processes leading to astrogliosis. It is suggestive from our findings that one mechanism of kolaviron therapy is in abolishing molecular inflammatory processes that occurred via induction of detoxifying enzymes which then halted astrogliosis. It has been suggested that the molecular mechanisms underlying the protective action of kolaviron are activated by suppressing certain proinflammatory genes whose expression have been shown to be regulated by transcription factors (Farombi et al., 2009).

Differential densities of microtubule associated proteins (MAPT and MAP2)

MAPT and MAP2 stabilize microtubules; by shifting neuronal reaction kinetics in favor of addition of new subunits, thereby accelerating microtubule growth and by binding to the outer surface of the microtubule protofilaments (Howard and Hyman, 2007). In similarity with the increment of MAPT density found in this study, expression of the tau gene, alternative splicing of its mRNA and its post-translational modification can modulate the normal architecture and functions of neurons as well as in situations of tauopathies, such as Alzheimer's disease (Wang and Liu, 2008). This further elucidates that a process involved in the observed neuronal apoptosis and axonal damage recorded in this study is the upregulated levels of tau protein. Oxidative stress such as induced by NaN_3 has been shown to affect the regulation of the neuronal cytoskeleton through regulatory mechanisms, including changes in expression levels, post-translational modifications and the effects of the binding of partner proteins (Wang and Liu, 2008), with some changes being protective and others pathogenic (Gardiner et al., 2013). Thus, the observed NaN_3-induced increase MAPT density in this study may be directly correlated to disturbances in mitochondrial biochemical redox ultimately resulted in oxidative stress.

Surprisingly, in contrast to the increased mean band density of MAPT associated with NaN_3-induced neurodegeneration in this study, there was a significant reduction in the mean band density of MAP2 in the PFC following NaN_3 administration. MAP2 deposition was highest in the CO, KV and KV+ NaN_3 groups while the mean densities of MAP2 in the NaN_3 and NaN_3+KV groups showed significant decreases when compared with the other three groups. This result is a bit intriguing, given that the observed MAPT densities is almost completely opposite MAP2 densities across the treatment groups especially since both proteins are microtubule associated. However, both aggregation and dissociation of MAPs can be forms of degenerative changes as shown by previous studies (Cartelli et al., 2010; Gardner et al., 2011) and buttressed by the observed degenerated axons and dendrites of neurons in the NaN_3-treated rats (since MAPT are found mostly in axons and MAPT in the dendrites) in this study (Cairns et al., 2004). The downregulation of MAP2 found in the NaN_3-treated rats in this study may also be as a result of oxidative stress and mitochondrial dysfunction. We published previously that NaN_3 dissociated light chain neurofilament (NFL) assembly (Olajide et al., 2015), the mechanism involved may include Tau dysregulation as NFL have been shown to directly bind microtubules, promote nucleation and prevent disassembly, and to induce the formation of parallel array (Mandelkow and Mandelkow, 1995). Similar to the protective mechanism of Kv against MAPT aggregation, its protective effect against MAP2 depolymerisation in the group of rats that received it before NaN_3 treatment was significant ($p<0.05$) as opposed to kolaviron-restorative effect observed in the group that received it after NaN_3-induced depletion of MAP2. Kv's potential to reduce background levels of protein oxidation

(Farombi et al., 2004) may explain the neutralization effect it has on mitochondrial-stress-related oxidative phosphorylation of MAPT and MAP2 induced by NaN_3 in this study.

Molecular role of NO in NaN_3-induced oxidative stress and mechanisms of Kolaviron intervention

In similarity to the neurotoxic processes leading to morphological alterations induced by NaN_3 discussed so far, there is evidence that NO may be one reactive radical that is involved in such degenerative cascades leading to neuronal cell death (Chung and David, 2010).

The overexpression of the studied isoforms of NOS by NaN_3 evinces the involvement of excessive production of NO radical in the earlier seen neuronal degeneration in this group, and also the inhibitive role of Kv further demonstrated its neuroprotective mechanisms. It has been discussed that NOS isoforms, particularly the inducible and neuronal types undertake unique roles during neuronal toxicity (Parathath et al., 2007). The specific NOS isoform activated during disease can determine how the NO produced promotes degeneration or neuroprotection (Zhou and Zhu, 2009). It was found that nNOS is critical for the progression of kainate-stimulated neurodegeneration and its activation in a model of focal ischemia was reported to promote neurotoxicity (Bal-Price and Brown, 2001); iNOS produces large amounts of NO as a defense mechanism during neural toxicity in response to cytokines while glia also produces NO primarily through the induction of iNOS (Bal-Price and Brown, 2001). In general, iNOS is considered responsible for the high output of NO in pathological, inflammatory central nervous system states. However, the involvement of both NOS isoforms in NaN_3-induced neurodegeneration and Kv neuroprotective mechanism by their inhibition is clearly elucidated by NOS immunoexpression in this study.

It has been shown that cytokines can additionally be produced by activated astrocytes, which may again respond to them by iNOS induction (Kuang et al., 2009). Thus, the neuroprotective mechanism of kolaviron against NaN_3-induced astrogliosis earlier observed in this study may contribute to the normoregulation of iNOS levels seen in the DLPFC of this group of rats. Furthermore, Quincozes-Santos et al. (2013) related overexpressed NOS to cellular changes similar to NaN_3-induced astrogliosis, alteration in cytoskeletal proteins and activation of apoptotic pathway proteins found in this study. Inhibition of NOS overexpression may therefore explain further, the mechanism by which Kv protected against these degenerative changes.

Kolaviron prevented NaN_3-induced neuronal apoptosis through inhibition of cell cycle dysregulation

Neuronal cell death is the major contributor to the neuropathology underlying a variety of degenerative diseases of the brain (Cordeiro et al., 2010; Lanni et al., 2012). The rational potential development of target-based strategy of Kv explored in this study against NaN_3-induced neurodegeneration was examined through demonstration of cell cycle regulatory proteins involved in the molecular mechanisms of apoptosis.

The roles of Bax

The expression of this protein was increased by NaN_3 administration when compared with the other groups in this study. This suggests that the neuronal apoptosis induced by NaN_3 in the DLPFC observed in H&E is through p53-mediated apoptotic pathways, as cellular expression of Bax is upregulated by p53 (Xiang et al., 1998). However, it was revealed that a mechanism by which Kv prevented neuronal cell death in this study is through inhibition of Bax. It has been discussed that in neurons a wide variety of death stimuli like oxidative stress are associated with Bax translocation in mitochondria followed by caspase activation (Dargusch et al., 2001). The antiapoptotic potentials of Kv shown in this study may be explained by the downregulation of Bax, as neurons lacking Bax are protected against apoptosis induced by growth factor deprivation and axotomy (Culmsee and Mattson, 2005). Furthermore, it has been shown that Bax deficiency results in the elimination of developmental cell death in many neuronal populations in the nervous system (Mattson, 2000).

Cathepsin D (CAD) is not involved in NaN_3-induced neuronal apoptosis

The cellular levels of CAD, which is a proteolytic enzyme, is one of the many molecular mechanisms that strictly regulate apoptosis (Minarowska et al., 2007). Surprisingly, CAD did not show any significant difference in mean band densities across treatment groups in this study. This suggests that this lysosomal protease is not involved in the mechanisms of NaN_3 induced neuronal apoptosis. The observed unaltered CAD levels despite changes in Bax levels is quite surprising, as several literatures indicated the involvement of CAD in p53-Bax mediated-apoptotic pathways, especially in neuronal death involving DNA oxidative damage. However, it has also been shown that not all models of apoptosis implicate the role of cathepsins. Some experiments with cathepsin inhibitors have demonstrated caspase-dependent apoptosis (Sarin et al., 1996).

The involvement of BCL-2 in neuronal apoptosis and Kolaviron therapy

Reports have implicated the Bcl-2 gene with antiapoptotic properties in neurodegenerative conditions (Nuydens et al., 2000). To assess and correlate its involvement/role in NaN_3-induced neuronal

apoptosis and to further elucidate the protective mechanisms of Kv, levels of the BCL-2 protein was demonstrated in the DLPFC of rats. Surprisingly, NaN_3 also increased BCL-2 levels, but in almost the same manner that it mediated the pro-apoptotic proteins upregulation; Kv pre-administration significantly prevented NaN_3-induced neuronal BCL-2 increment. Safe for the earlier observed degenerative changes in the DLPFC of rats associated with NaN_3 treatment in this study, the upregulation of BCL-2 gene normally translates for anti-apoptotic activities within neurons. It has been shown, for example, that upregulated Bcl-2 in cell culture and transgenic mice increases resistance of neurons to death during development, and protects from apoptosis induced by excitotoxic, metabolic and oxidative insults relevant to AD, stroke and other NDDs (Stefanis et al., 1997). However, Marshall et al. (1997) showed that Bcl-2 was significantly raised in the basal ganglia regions of PD and Lewy body disease patients as compared to age-matched control. This report is in line with the neurodegenerative-related Bcl-2 increment observed in this study, as they also proposed that Bcl-2 increase in some brain regions are early event associated with neurodegeneration, especially those caused by oxidative stress. In addition, the expression of both Bcl-2 and Bax is regulated by the p53 tumor suppressor gene (Miyashita and Reed, 1995), therefore the irregularity observed in the p53 apoptotic pathway induced by NaN_3 may explain the complimentary Bcl -2 overexpression.

Conclusion

Kolaviron exhibited significant neuroprotective properties against NaN_3-orchestrated degenerative changes, by inhibiting or slowing the dysfunction of molecular players necessary for normal neuronal integrity and health. The main neuroprotective mechanisms underlying kolaviron therapeutic measures against neuronal apoptosis shown in this study include; maintenance and inhibition of excess NO production, normoregulation of neuronal cytoskeletal and supporting proteins (especially those necessary for maintaining axonal and dendritic integrity), and suppressing the uprising levels of cell death proteins within neurons. However, the neuroprotective effect of kolaviron was observed to be significantly higher when it was administered before NaN_3 treatment than after NaN_3 treatment.

ACKNOWLEDGEMENTS

The authors wish to thank Dr. Stephen Price of the Research Department of Cell and Developmental Anatomy, University College London, London, Britain. His laboratory hosted a significant part of this study under the ISN/CAEN Category 1C grant award. Also, the International Society for Neurochemistry is acknowledged for supporting this work with the ISN-CAEN 1A grants awarded to OLAJIDE, Olayemi Joseph.

LIST OF ABBREVIATIONS

CO – Corn oil
KV – Kolaviron only
NaN3 – Sodium azide only
NaN3+KV – Sodium azide then Kolaviron
KV+NaN3 – Kolaviron then Sodium azide
H&E – Haematoxylin and Eosin
GFAP – Glia fibriliary acidic protein
iNOS – Inducible nitric oxide synthase
nNOS – Neuronal nitric oxide synthase
MAPT – Microtubule associated protein Tau
MAP2 - Microtubule associated protein 2
BCL2 – B-cell lymphoma 2
Bax - B-cell lymphoma associated protein X
CAD – Cathepsin D
GAPDH – Glyceraldehyde phosphate dehydrogenase

REFERENCES

ADARAMOYE OA, NWANERI VO, ANYANWO KC, FAROMBI EO, EMEROLE GO (2005) Possible anti-atherogenic effect of kolaviron (a Garcinia kola seed extract) in hypercholesterolaemic rats. *Clin Exp Pharmacol Physiol*, 32: 40-46.

AHMED MAE, FAROUK FAHMY H (2013) Histological study on the effect of sodium azide on the corpus striatum of albino rats and the possible protective role of L-carnitine. *Egypt J Histol*, 36: 39-49. Available from http://content.wkhealth.com/linkback/openurl?sid=WKPTLP:landingpage&an=00767537-201303000-00004

BAL-PRICE A, BROWN GC (2001) Inflammatory neurodegeneration mediated by nitric oxide from activated glia- inhibiting neuronal respiration, causing glutamate release and excitotoxicity. *J Neurosci*, 21(17): 6480-6491.

BUFFO A, RITE I, TRIPATHI P, LEPIER A, COLAK D, HORN A-P, MORI T, GÖTZ M (2008) Origin and progeny of reactive gliosis: A source of multipotent cells in the injured brain. *Proc Natl Acad Sci USA*, 105(9): 3581-3586.

CAIRNS NJ, LEE VMY, TROJANOWSKI JQ (2004) The cytoskeleton in neurodegenerative diseases. *J Pathol*, 204(4): 438-449.

CARTELLI D, RONCHI C, MAGGIONI MG, RODIGHIERO S, GIAVINI E, CAPPELLETTI G (2010) Microtubule dysfunction precedes transport impairment and mitochondria damage in MPP+-induced neurodegeneration. *J Neurochem*, 115(1): 247-258.

CECIL KM, BRUBAKER CJ, ADLER CM, DIETRICH KN, ALTAYE M, EGELHOFF JC, WESSEL S, ELANGOVAN I, HORNUNG R, JARVIS K, LANPHEAR BP (2008) Decreased brain volume in adults with childhood lead exposure. *PLoS Med*, 5(5): 0741-0749.

CHANG J, YANG JY, CHOI J, JUNG HH, IM GJ (2011) Calcium imaging in gentamicin ototoxicity: Increased intracellular calcium relates to oxidative stress and late apoptosis. *Int J Pediatr Otorhinolaryngol*, 75(12): 1616 -1622.

CHUNG KK, DAVID KK (2010) Emerging roles of nitric oxide in neurodegeneration. *Nitric Oxide*, 22(4): 290-295.

CLARKE LE, BARRES BA (2013) Emerging roles of astrocytes in neural circuit development. *Nat Rev Neurosci*, 14(5): 311-321. Available from: http://www.ncbi.nlm.nih.gov/pubmed/23595014

COLEMAN MP, FREEMAN MR (2010) Wallerian degeneration, wld(s), and nmnat. *Annu Rev Neurosci*, 33: 245-267.

CORDEIRO MF, GUO L, COXON KM, DUGGAN J, NIZARI S, NORMANDO EM, SENSI SL, SILLITO AM, FITZKE FW, SALT TE, MOSS SE (2010) Imaging multiple phases of neurodegeneration: a novel approach to assessing cell death in vivo. *Cell Death Dis*, 1: e3.

COWARD LA (2013) Neuron Physiology. Towards a Theoretical Neuroscience: from Cell Chemistry to Cognition. Vol. 8 Springer Series in Cognitive and Neural Systems pp 53-95. Available from: http://link.springer.com/chapter/10.1007/978-94-007-7107-9_4

CULMSEE C, MATTSON MP (2005) P53 in neuronal apoptosis. *Biochem Biophys Res Commun*, 331(3): 761-777.

DARGUSCH R, PIASECKI D, TAN S, LIU Y, SCHUBERT D (2001) The role of Bax in glutamate-induced nerve cell death. *J Neurochem*, 76(1): 295-301.

DE VOS KJ, GRIERSON AJ, ACKERLEY S, MILLER CCJ (2008) Role of axonal transport in neurodegenerative diseases. *Annu Rev Neurosci*, 31: 151-173.

EBRAHIMI-FAKHARI D, WAHLSTER L, MCLEAN PJ (2012) Protein degradation pathways in Parkinson's disease: Curse or blessing. *Acta Neuropathol*, 124(2): 153-172.

ELMORE S (2007) Apoptosis: a review of programmed cell death. *Toxicol Pathol*, 35(4): 495-516.

ENCIU AM, NICOLESCU MI, MANOLE CG, MUREŞANU DF, POPESCU LM, POPESCU BO (2011) Neuroregeneration in neurodegenerative disorders. *BMC Neurol*, 11: 75.

FAROMBI EO, OWOEYE O (2011) Antioxidative and chemopreventive properties of Vernonia amygdalina and Garcinia biflavonoid. *Intl J Environ Res Public Health*, 8(3): 2533-2555.

FAROMBI EO, HANSEN M, RAVN-HAREN G, MØLLER P, DRAGSTED LO (2004) Commonly consumed and naturally occurring dietary substances affect biomarkers of oxidative stress and DNA damage in healthy rats. *Food Chem Toxicol*, 42: 1315-1322.

FAROMBI EO, SHROTRIYA S, SURH YJ (2009) Kolaviron inhibits dimethyl nitrosamine-induced liver injury by suppressing COX-2 and iNOS expression via NF-??B and AP-1. *Life Sci*, 84: 149-155.

FAROMBI EO, ADEDARA IA, AJAYI BO, AYEPOLA OR, EGBEME EE (2013) Kolaviron, a natural antioxidant and anti-inflammatory phytochemical prevents dextran sulphate sodium-induced colitis in rats. *Basic Clin Pharmacol Toxicol*, 113: 49-55.

FARZAN F, BARR MS, LEVINSON AJ, CHEN R, WONG W, FITZGERALD PB, DASKALAKIS ZJ (2010) Evidence for gamma inhibition deficits in the dorsolateral prefrontal cortex of patients with schizophrenia. *Brain*, 133(5): 1505-1514.

FRIEDLANDER RM (2003) Apoptosis and caspases in neurodegenerative diseases. *N Engl J Med*, 348(14): 1365-1375.

FRITSCHY JM, HARTIG W (1999) Immunofluorescence. *Encycl Life Sci*, 1-7. http://doi.org/10.1038/npg.els.0001174

GARDNER MK, ZANIC M, GELL C, BORMUTH V, HOWARD J (2011) Depolymerizing kinesins Kip3 and MCAK shape cellular microtubule architecture by differential control of catastrophe. *Cell*, 147(5): 1092-1103.

GARDINER J, OVERALL R, MARC J (2013) The nervous system cytoskeleton under oxidative stress. *Diseases*, 1(1): 36-50. Available from: http://www.mdpi.com/2079-9721/1/1/36/

HOWARD J, HYMAN AA (2007) Microtubule polymerases and depolymerases. *Curr Opin Cell Biol*, 19(1): 31-35.

IGADO OO, OLOPADE JO, ADESIDA A, AINA OO, FAROMBI EO (2012) Morphological and biochemical investigation into the possible neuroprotective effects of kolaviron (Garcinia kola bioflavonoid) on the brains of rats exposed to vanadium. *Drug Chem Toxicol*, 35: 371-380. Available from: <Go to ISI>://WOS:000308936500004

IWU MM (1985) Antihepatoxic constituents of Garcinia kola seeds. *Experientia*, 41: 699-700.

JOSEPH J, COLE G, HEAD E, INGRAM D (2009) Nutrition, brain aging, and neurodegeneration. *J Neurosci*, 29(41): 12795-12801.

KIERNAN J, LILLIE R, PIZZOLATO P, DONALDSON P, LLEWELLYN B, PUCHTLER H, WALDROP F (2010) Haematoxylin Eosin (H&E) staining Protocols Online. p. 1-1. Available from: file:///home/ostedham/Desktop/Haematoxylin Eosin (H&E) staining%C2%A0 %C2%A0Protocols Online.html

KUANG X, SCOFIELD VL, YAN M, STOICA G, LIU N, WONG PKY (2009) Attenuation of oxidative stress, inflammation and apoptosis by minocycline prevents retrovirus-induced neurodegeneration in mice. *Brain Res*, 1286: 174-184.

LANNI C, RACCHI M, MEMO M, GOVONI S, UBERTI D (2012) p53 at the crossroads between cancer and neurodegeneration. *Free Radic Biol Med*, 52(9): 1727-1733.

LIU B, CHE W, ZHENG C, LIU W, WEN J, FU H, TANG K, ZHANG J, XU Y (2013) SIR T5: A safeguard against oxidative stress- induced apoptosis in cardiomyocytes. *Cell Physiol Biochem*, 32(4): 1050-1059.

LUQUES L, SHOHAM S, WEINSTOCK M (2007) Chronic brain cytochrome oxidase inhibition selectively alters hippocampal cholinergic innervation and impairs memory□: Prevention by ladostigil. *Exp Neurol*, 206:

209-219.

MAJOR G, LARKUM ME, SCHILLER J (2013) Active properties of neocortical pyramidal neuron dendrites. *Annu Rev Neurosci*, 36: 1-24. Available from: http://www.ncbi.nlm.nih.gov/pubmed/23841837

MANDELKOW E, MANDELKOW EM (1995) Microtubules and microtubule-associated proteins. *Curr Opin Cell Biol*, 7(1): 72-81.

MARINO S, MARANI L, NAZZARO C, BEANI L, SINISCALCHI A (2007) Mechanisms of sodium azide-induced changes in intracellular calcium concentration in rat primary cortical neurons. *Neurotoxicology*, 28(3): 622-629.

MARSHALL KA, DANIEL SE, CAIRNS N, JENNER P, HALLIWELL B (1997) Upregulation of the anti-apoptotic protein Bcl-2 may be an early event in neurodegeneration: studies on Parkinson's and incidental Lewy body disease. *Biochem Biophys Res Commun*, 240(1): 84-87.

MATTSON MP (2000) Apoptosis in neurodegenerative disorders [Review]. *Nat Rev Mol Cell Biol*, 1(2): 120-129.

MEGYERI K, ALBERT M, KOMPAGNE H (2008) A new treatment regime for sodium azide to evoke experimental Alzheimer's disease for pharmacological screening. *Meas Behav*, 208: 4-5.

MERCER RE, KWOLEK EM, BISCHOF JM, VAN EEDE M, HENKELMAN RM, WEVRICK R (2009) Regionally reduced brain volume, altered serotonin neurochemistry, and abnormal behavior in mice null for the circadian rhythm output gene Magel2. *Am J Med Genet Part B Neuropsychiatr Genet*, 150(8): 1085-1099.

MINAROWSKA A, MINAROWSKI Ł, KARWOWSKA A, GACKO M (2007) Regulatory role of cathepsin D in apoptosis. *Folia Histochem Cytobiol*, 45(3): 159-163.

MIYASHITA T, REED JC (1995) Tumor suppressor p53 is a direct transcriptional activator of the human bax gene. *Cell*, 80(2): 293-299.

NAVARRO A, BOVERIS A (2010) Brain mitochondrial dysfunction in aging, neurodegeneration, and Parkinson's disease. *Front Aging Neurosci*, 2: 34.

NIEOULLON A (2011) Neurodegenerative diseases and neuroprotection: current views and prospects. *J Appl Biomed*, 9(4): 173-183. http://doi.org/10.2478/v10136-011-0013-4

NUYDENS R, DISPERSYN G, VAN DEN KIEBOOM G, DE JONG M, CONNORS R, RAMAEKERS F, BORGERS M, GEERTS H (2000) Bcl-2 protects against apoptosis-related microtubule alterations in neuronal cells. *Apoptosis*, 5(1): 43-51.

OLAJIDE OJ, ENAIBE BU, BANKOLE OO, AKINOLA OB, LAOYE BJ, OGUNDELE OM (2015) Kolaviron was protective against sodium azide (NaN_3) induced oxidative stress in the prefrontal cortex. *Metab Brain Dis*. Available from: http://link.springer.com/10.1007/s11011-015-9674-0

OLALEYE SB, FAROMBI EO (2006) Attenuation of indomethacin- and HCl/ethanol-induced oxidative gastric mucosa damage in rats by kolaviron, a natural biflavonoid of Garcinia kola seed. *Phyther Res*, 20: 14-20.

OSTEN P, MARGRIE TW (2013) Mapping brain circuitry with a light microscope. *Nat Methods*, 10(6): 515-523. Available from: http://www.pubmedcentral.nih.gov/articlerender.fcgi?artid=3982327&tool=pmcentrez&rendertype=abstract

PARATHATH SR, PARATHATH S, TSIRKA SE (2006) Nitric oxide mediates neurodegeneration and breakdown of the blood-brain barrier in tPA-dependent excitotoxic injury in mice. *J Cell Sci*, 119(Pt 2): 339-349.

PARATHATH SR, GRAVANIS I, TSIRKA SE (2007) Nitric oxide synthase isoforms undertake unique roles during excitotoxicity. *Stroke*, 38(6): 1938-1945.

QUINCOZES-SANTOS A, BOBERMIN LD, LATINI A, WAJNER M, SOUZA DO, GONÇALVES CA, GOTTFRIED C (2013) Resveratrol protects C6 astrocyte cell line against hydrogen peroxide-induced oxidative stress through heme oxygenase 1. *PLoS One*, 8(5): e64372.

ROLLS A, SHECHTER R, SCHWARTZ M (2009) The bright side of the glial scar in CNS repair. *Nat Rev Neurosci*, 10(3): 235-241.

RUBINSZTEIN DC (2006) The roles of intracellular protein-degradation pathways in neurodegeneration. *Nature*, 443: 780-786.

SARIN A, WU ML, HENKART PA (1996) Different interleukin-1 beta converting enzyme (ICE) family protease requirements for the apoptotic death of T lymphocytes triggered by diverse stimuli. *J Exp Med*, 184(6): 2445-2450.

SCHLAEPFER TE, LANCASTER E, HEIDBREDER R, STRAIN EC, KOSEL M, FISCH HU, PEARLSON GD (2006) Decreased frontal white-matter volume in chronic substance abuse. *Int J Neuropsychopharmacol*, 9(2): 147-153.

SMITH RP, LOUIS CA, KRUSZYNA R, KRUSZYNA H (1991) Acute neurotoxicity of sodium azide and nitric oxide. *Toxicol Sci*, 17(1): 120-127.

SOFRONIEW MV (2009) Molecular dissection of reactive astrogliosis and glial scar formation. *Trends Neurosci*, 32(12): 638-647.

STEFANIS L, BURKE RE, GREENE LA (1997) Apoptosis in neurodegenerative disorders. *Curr Opin Neurol*, 10(4): 299-305.

SU B, WANG X, LEE H-G, TABATON M, PERRY G, SMITH MA, ZHU X (2010) Chronic oxidative stress causes increased tau phosphorylation in M17 neuroblastoma cells. *Neurosci Lett*, 468(3): 267-271.

SU K, BOURDETTE D, FORTE M (2013) Mitochondrial dysfunction and neurodegeneration in multiple sclerosis. *Front Physiol*, 4: 169.

SZABADOS T, DUL C, MAJTÉNYI K, HARGITAI J, PÉNZES Z, URBANICS R (2004) A chronic Alzheimer's model evoked by mitochondrial poison sodium azide for pharmacological investigations. *Behav Brain Res*, 154: 31-40.

TRIOLO D, DINA G, LORENZETTI I, MALAGUTI M, MORANA P, DEL CARRO U, COMI G, MESSING A, QUATTRINI A, PREVITALI SC (2006) Loss of glial fibrillary acidic protein (GFAP) impairs Schwann cell proliferation and delays nerve regeneration after damage. *J Cell Sci*, 119(Pt 19): 3981-3993.

TRUSHINA E, MCMURRAY CT (2007) Oxidative stress and mitochondrial dysfunction in neurodegenerative diseases. *Neuroscience*, 145(4): 1233-1248.

VAN LAAR VS, BERMAN SB (2013) The interplay of neuronal mitochondrial dynamics and bioenergetics: Implications for Parkinson's disease. *Neurobiol Dis*, 51: 43-55.

WANG CX, SONG JH, SONG DK, YONG VW, SHUAIB A, HAO C (2006) Cyclin-dependent kinase-5 prevents neuronal apoptosis through ERK-mediated upregulation of Bcl-2. *Cell Death Differ*, 13(7): 1203-1212.

WANG JZ, LIU F (2008) Microtubule-associated protein tau in development, degeneration and protection of neurons. *Prog Neurobiol*, 85(2): 148-175.

XIANG H, KINOSHITA Y, KNUDSON CM, KORSMEYER SJ, SCHWARTZKROIN PA, MORRISON RS (1998) Bax involvement in p53-mediated neuronal cell death. *J Neurosci*, 18(4): 1363-1373.

ZHANG D, HU X, QIAN L, O'CALLAGHAN JP, HONG JS (2010) Astrogliosis in CNS pathologies: Is there a role for microglia? *Mol Neurobiol*, 41(2-3): 232-241.

ZHOU L, ZHU DY (2009) Neuronal nitric oxide synthase: structure, subcellular localization, regulation, and clinical implications. *Nitric Oxide*, 20(4): 223-230.